Desalination and Water Treatment
www.deswater.com

doi:10.5004/dwt.2018.22093

125 (2018) 116–123
September

The research on new technology and separation performance of wastewater treatment for offshore field

Z.G. Zhao[a,*], M.Q. Feng[b], J.G. Liu[a], Y.K. Tao[a], J.S. Wang[a], L. Wang[a], G.Q. Peng[b]

[a]*Jiangsu key laboratory of traffic and transportation security, Huaiyin Institute of Technology, SE-223001 Huaian, China, email: 51066347@qq.com (Z.G. Zhao), 874526230@qq.com (J.G. Liu), 576659612@qq.com (Y.K. Tao), 1305634523@qq.com (J.S. Wang), 792245610@qq.com (L. Wang)*
[b]*Collegel of Mechanical and Power Engineering, Nanjing Tech University, SE-210000 Nanjing, China, email: 1369742018@qq.com (M.Q. Feng), 714602865@qq.com (G.Q. Peng)*

Received 31 January 2018; Accepted 20 February 2018

ABSTRACT

Wastewater treatment and recycling for offshore oilfield can bring economic and social benefits. This paper produced wastewater treatment and recycling technological process for offshore oilfield combining with engineering practice. Considering the complexity of internal flow in disc separator, VOF model and RNG *k*-ε turbulence model were used to numerically simulate the process of separating oil-water in the separator then the law of distribution and the efficiency of separating oil-water such as flow velocity, pressure, turbulent kinetic energy, turbulent flow, laminar flow and so on were obtained. The discrete phase model (DPM) was used to simulate the motion of particles, then obtained the motion process and separation efficiency of discrete phase particles. The test results show that, the separation efficiency of the calculation and actual measurements both meet the design requirements with the separation efficiency calculated slightly higher than that in the actual measurements. The relative error of oil-water separation efficiency and particle separation efficiency are 1.5% and 1.4% respectively. The data indicate that the numerical simulation method is reliable for predicting the separation performance of the separator, so wastewater treatment and recycling technological process meet the requirements of engineering application.

Keywords: Wastewater treatment; Technological process; Oil-water separation; Disc separator; Separation performance

1. Introduction

With the increasing demand for energy and the increasing development of offshore oilfield, oil fields have been producing a large number of oil produced sewage during the process of development, and these sewage have been irrationally abandoned, which is not only a great waste of energy but also a serious pollution to the water, soil and air [1]. Therefore, recovery and reusing oilfield wastewater have good economic and social benefits.

The problem of recycling oilfield wastewater has always been of great concern by developed countries in Europe, and the United States is the earliest country to propose recycling. The technology of regenerating oilfield wastewater is mainly divided into three types [2–5]. The first type is reclamation process, and it contains sedimentation, centrifugation, filtration and flocculation. The second type is reprocessing process, which is adsorption refining or chemical refining based on the re purification process. The third type is re refining process, including distillation, sulfuric acid and clay technology.

The disc separator is used to remove oil and impurities from wastewater. It can reduce the pollution of oceans by recovery and reusing oilfield wastewater. Zhao [6], Wang [7], Xue [8] and more studied on the performance of disc separator. Zhao [6], Shi [9], Li [10], Wu [11], Tang [12] and more have done a lot of research on two-dimensional and three-dimensional flow field.

*Corresponding author.

A technique of recycling wastewater in offshore oilfield was designed combining with engineering practice. In view of the complexity of internal flow in disc separator, the unsteady numerical simulation of the internal flow in separator was carried out by choosing the multi-phase flow model, the turbulence model and the discrete phase model. The process of separating oil-water-solid, the track of particle motion and the separating efficiency were analyzed. Compared with the test results, this method provides a new way for recycling wastewater in offshore oil field, and also gives the basis for the development and optimal design on the virtual prototype of the separator. Meanwhile, it also reduces the experimental time and the costs of product development.

2. Recycling technology of wastewater in offshore oilfield

The composition of oilfield wastewater is complex, and the oil content and the existence form of oil in the water are different, so the single treatment method is often ineffective. In practical application, two or three methods are usually used in combination, which meet the discharge standards. The treated oil contains a small amount of water and impurities after preliminary treatment. This paper focuses on the process of removing water and impurity from the oil.

The installation of recycling technological process of wastewater in offshore oilfield is mainly composed of disc separator, automatic filter, heater, adsorption filter, oil quality monitor and so on.

The wastewater stored in the waste tank is transported to the automatic filter through the pump, then the automatic filter removes the large diameter particles, and reduces the viscosity of oil to improve the separation effect of disc separator under heating action of the heater. The disc separator uses different densities of oil, water and other impurities in the spent oil to obtain different centrifugal forces, so the wastewater in the disc separation zone of separator drum can be separated. The separated purified oil is exported to core pump by the light phase, the water is exported to core pump by the heavy phase, and the impurities are deposited on the inner surface of the drum. The impurities are discharged out of the machine regularly through the controlling of the operating water to the deslagging operation of barrate. The recycling technological process of oilfield wastewater is shown as Fig. 1.

As the core component of recycling oilfield wastewater, disc separator is mainly used to re-texture spent oil, remove moisture and mechanical impurities. As shown in Fig. 2.

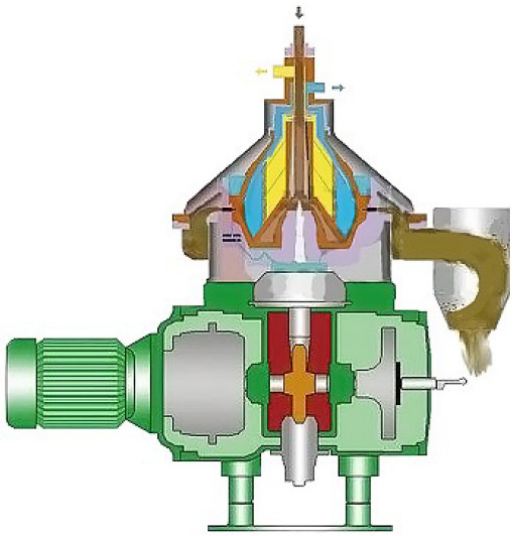

Fig. 2. Schematic of disc separator.

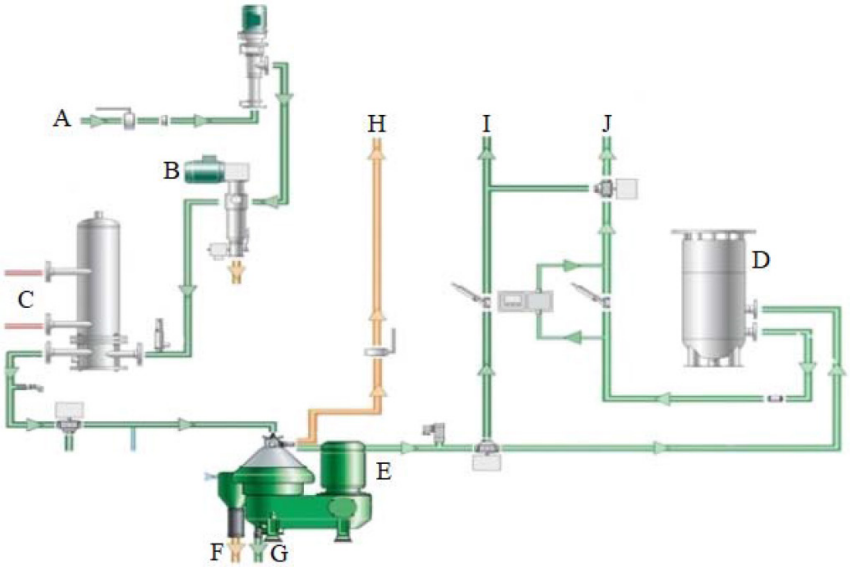

Fig. 1. Recycling technological process of oilfield wastewater A-Wastewater inlet, B-Automatic filter, C-Heater, D-Adsorption filter, E-Disc separator, F-Impurity outlet, G-Operating water outlet, H-Purified oil outlet, I-Effluent oil reflux inlet, J-Clean water outlet.

3. Fluid dynamics governing equations

3.1. Fluid control equations for oil-water separation

Fluid control equations for oil-water separation include continuity equation, momentum equation, energy equation, component equation, turbulent kinetic energy *k* equation and turbulent dissipation rate ε equation. These governing equations all can be expressed as the following general form [6].

$$\frac{\partial \rho\phi}{\partial t} + div(\rho u\phi) = div(\Gamma grad\phi) + S \tag{1}$$

The expanded form is

$$\frac{\partial(\rho\phi)}{\partial t} + \frac{\partial(\rho u\phi)}{\partial x} + \frac{\partial(\rho v\phi)}{\partial y} + \frac{\partial(\rho w\phi)}{\partial z} = \frac{\partial}{\partial x}(\Gamma\frac{\partial\phi}{\partial x}) + \frac{\partial}{\partial y}(\Gamma\frac{\partial\phi}{\partial y}) + \frac{\partial}{\partial z}(\Gamma\frac{\partial\phi}{\partial z}) + S \tag{2}$$

where ϕ is the generalized variables, Γ is the diffusion coefficient, *S* is the source term, and *u*, *v* and *w* (m/s) are the velocity in *x*, *y* and *z* directions respectively, ρ (kg/m^3) represents the density of oil-water mixture, which can be approximated with ρ = 900 kg/m^3, *t* (s) refers to the time.

3.2. Discrete phase control equations for solid separation

In a discrete phase, the position of the particle is tracked by calculating its acceleration, and motion equations are as follows [6].

$$\frac{dv_{p-i}}{dt} = F_{D-i}(v_i - v_{p-i}) + \frac{g_i(\rho_p - \rho)}{\rho_p} + F_d \tag{3}$$

where $\frac{dv_{p-i}}{dt}$ (N) is the inertia force of unit cell, *i* represents the three directions of *x*, *y*, *z*, $\frac{g_i(\rho_p - \rho)}{\rho_p}$ is the ratio between the buoyancy and gravity of unit cell, ρ_p (kg/m^3) is the density of particle, F_d (N) is the centrifugal force of particle, and $F_d = mw^2r$.

4. Flow field model and simulation settings

4.1. Physical modeling and meshing

Rotating parts in a separator drum are all symmetric. Instead of the 3D structure, the two-dimensional model with a defined rotating shaft is used in the Gambit software to simplify the calculation model. The triangle unstructured grid is used, as shown in Fig. 3. And the boundary conditions can be set by introducing the mesh model and the mesh file into Fluent.

The basic parameters of physical model are as follows. the width is 160 mm, the height is 165 mm, the inlet diameter is d = 16 mm, the number of discs is 52, the thickness of the discs is 0.4 mm, and the gap between the discs is 0.5 mm.

4.2. Boundary conditions

Velocity boundary condition is taken as the inlet boundary. Assuming that the axial velocity at the inlet boundary is uniform without tangential velocity and radial velocity. Therefore, the axial velocity is determined by the flow volume and the sectional area of the inlet, namely, the inlet velocity in the X direction is 1.38 m/s.

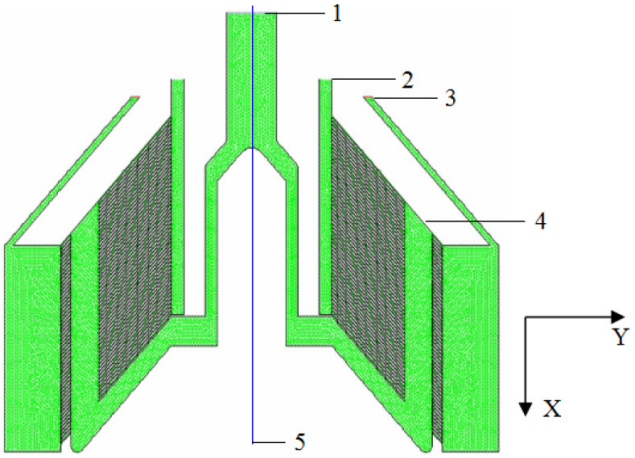

Fig. 3. Model of the disc-separator drum and the mesh generation 1-fluid inlet, 2-oil outlet, 3- water outlet,4- neutral aperture, 5- rotation axis.

Natural outflow boundary condition is taken as the outlet boundary, that is, "outflow" is the type of outlet and the rotation velocity of the wall is 847.4 rad/s. Non-slip condition is adopted on the solid wall of the computational area. Volumetric force is applied in the positive direction of the X axis, namely, the acceleration of gravity is 9.8 m/s^2. The heat produced by friction is neglected because temperature rises slightly during the whole process.

In order to calculate the separation efficiency of particles, it is necessary to distinguish the particles escaping from the water outlet and the oil outlet. The discrete phase boundary conditions are set as follows. the DPM boundary of the oil outlet is "trap" and that of the water outlet is "escape". The DPM boundary of the barrate wall and disc is "reflect", which means that the particles will be reflected if they touch the wall. Considering the influence of fluid turbulence on particle motion, the discrete phase is coupled with the continuous phase.

According to known conditions, the reynolds number R_e is 690, the turbulence intensity *I* is 1%, the turbulent kinetic energy is 0.000286 and the turbulent dissipation rate ε is 0.000708, which are obtained by papers [6].

4.3. Particle parameters

Rosin-Rammler distribution function can be used to describe the distribution of the particles. In Fluent, Rosin-Rammler model can be used to release particles, and its distribution function is [6,13].

$$F(d) = 1 - \exp\left[-\left(\frac{d_p}{d_{50}}\right)^m\right] \tag{4}$$

where $F(d)$ is a distribution function, d_{50} (μm) is the particle size when the cumulative weight distributes at $F = 0.5$, namely medien diameter, and *m* is the propagation coefficient.

When d_{50} and m are both determined, the distribution of the particle is uniquely determined also. To define variable Y_d as the mass fraction of those particles larger than the specified size d within the proper ranges of particle size, and then the particle diameters and the particle distribution corresponding to accumulated mass fraction are shown in Table 1.

When $Y_d = 100e^{-1} = 38.6$, the corresponding d value is d_{50}. Since there is no 38.6 in Table 1, it is necessary to fit the existing values to obtain the curve, d is 21 μm when Y_d = 38.6, that is d_{50} = 21 μm.

The propagation coefficient m is

$$m = \frac{\ln\left(-\ln Y_d\right)}{\ln\left(\frac{d}{d_{50}}\right)} \tag{5}$$

The propagation coefficient m of different particle diameters can be obtained based on the known d, Y_d and d_{50}.

The separation efficiency of mechanical impurities is an important evaluation index for disc separator. When applying DPM model, it is necessary to set the particle mass flow at the inlet, which should be

$$M_0 = 0.3\% M \quad M = \pi r^2 v_0 \rho_1 \tag{6}$$

where M (kg/s) refers to the mass flow rate in the mixture at the inlet, M_0 (kg/s) is the mass flow rate of particles at the inlet, ρ_1 (kg/m^3) is the density of mixture, R (m) is the inlet radius, and v_0 (m/s) is the inlet velocity.

It can be obtained that M_0 = 0.000708 kg/s from known conditions.

The particle size distributions of particulate impurities range from 2 μm to 100 μm unevenly, and particle size distribution are described in the discrete phase model. Rosin-Rammler model is taken to release particles at the inlet. The inlet releases 16 groups with 100 beams in each group at every 0.0001s, totaling 20 times with 32, 000 particles, and the particle parameter settings are shown in Table 2.

4.4. Multiphase flow model and algorithm

The VOF model is adopted in the separation of oil and water, and the separator is of a strong turbulence at high speed rotation, therefore the RNG k-ε turbulence model is used in calculation. The turbulence model is of better stability, economy and accuracy. Wall function method is adopted in wall region. The unsteady and incompressible Reynolds averaged N-S equation is used as the governing equation for the incompressible oil-water mixture, the partial turbulence in the separator and the internal changing pressure. The DPM is used to simulate the motion of particles in the oil-water-solid separation, and the particle trajectory of discrete phase can be obtained by Lagrange method in the known flow field of oil and water continuous phase.

The SIMPLEC algorithm is applied to solve the governing equations, one-order central difference scheme is used for the pressure term in the discrete control equation, and one-order upwind difference scheme is adopted for the momentum equation, turbulent kinetic energy and turbulent dissipation equation. iterative computation of algebraic equations take under relaxation factors algorithm, whose defaults for pressure, momentum, K and ε are 0.2, 0.5, 0.5, 0.5 respectively. In Fluent, the defaults of under relaxation factors of all variables are the optimal value of most problems. There is no need to modify the default values for the majority of the flow, but it is necessary to reduce the under relaxation factors if the residual is still increasing after 4–5 iterations.

Table 1
Granule distributions of particle diameters and corresponding mass fraction

Particle size d/μm	Cumulative mass fraction Y_d/%	Propagation coefficient m
2	100.00	
5	91.06	1.65
15	57.54	1.81
25	27.53	1.38
50	4.19	1.35
100	0.02	1.42

5. Characteristics of Internal flow field

5.1. Oil-water separation

Before starting the separator, the outlet should be sealed with water to establish oil-water interface in case that the oil leaks from the outlet. In the initial state, the drum is filled with water, and the water in the raw material is 3%. The oil-water separation process is shown in Fig. 4.

It can be seen from Fig. 4 that the water gradually moves outwards by larger centrifugal force while the oil accumulates in the inner side and gradually moves to the outlet after entering into the disc neutral hole, and eventually the oil-water mixture forms the stable interface. By monitoring the oil content at the outlet and Fig. 4(d), it can be seen that the oil and water are separated generally with the oil volume fraction at outlet is close to 1 and the water removal rate is about 99.8%, indicating that the separator is of a great oil-water separation effect.

5.2. Particle separation and concentration distribution

Using the Discrete Phase in Fluent to simulate the trajectory of solid particles, whose motion is shown in Fig. 5

Table 2
Granule parameters

Smallest particle, μm	2
Largest particle, μm	100
Average particle size, μm	21
Propagation coefficient	1.5
Density, kg/m^3	5000
Mass flow rate at the inlet, kg/s	0.000708
Total mass at the inlet, kg	0.00000142

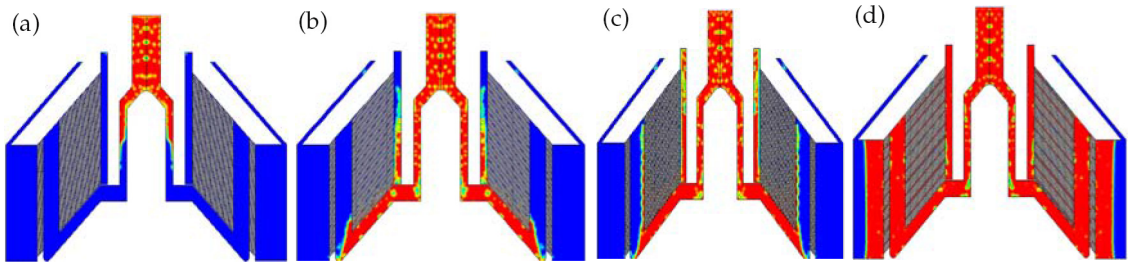

Fig. 4. The process of oil-water separation (a) The raw material is input into the feed tube, (b) Oil-water mixture is transmitted into the neutral aperture (c) Oil-water moves from the neutral aperture towards the two ends, (d) Oil-water separation forms the stable interface.

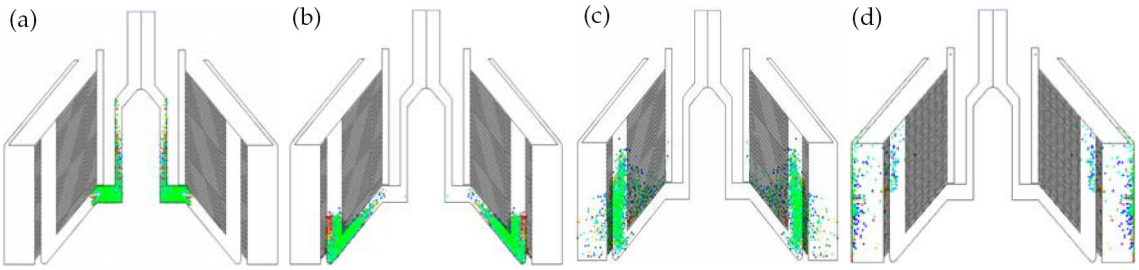

Fig. 5. Movement of droplets and concentration distribution (a) Droplets go into the feed tube, (b) Droplets go into the neutral aperture (c) Droplets move from the neutral aperture towards the two ends, (d) Droplets are finally pasted on the drum wall.

Fig. 5. shows that large particles mainly concentrate on the lower half of the disc group and distribute evenly with higher mass concentration. The large particles have been attached to the feed tube wall before entering the disc, then slide into the neutral hole along the wall, and the reason for this distribution is that the density of the large particle is larger than that of the liquid, which is significantly affected by the inertial and centrifugal force. After entering the neutral hole of the disc, the particles move toward both ends of the disc and most of the larger particles move toward the edge of disc with larger diameter, then there is a trend to gather particles toward the lower surface of the disc by centrifugal force after entering the disc. The greater the flow rate, the more obvious aggregation of the larger diameter particles, which were eventually deposited in the drum or discharged with waste water.

5.3. Velocity distribution

Gelijin makes the conclusion based on a lot of experiments that when $\lambda < 4$, the flow velocity distribution in the gap between discs is similar to the general parabola, and the maximum appears in the middle area of the discs while approximately approaching 0 near the wall. The λ value is 1.63 calculated from the known conditions, which is within the λ value ranges recommended by Gelijin and accords with the design requirements.

Fig. 6. shows the velocity distribution diagram when the stream field is stable.

From the speed distribution diagram in Fig. 6, the liquid velocity is distributed evenly in the drum and the whole symmetry of the drum is obvious. The flow velocity of the liquid changes with the increasing of the rotating speed of the drum, with an increasing trend from the rotating center to the edge of the drum, and reaches the maximum near the drum wall. Taking six cross sections along the radius R, namely, $y_1 = 30$ mm, $y_2 = 40$ mm, $y_3 = 50$ mm, $y_4 = 60$ mm, $y_5 = 70$ mm, and $y_6 = 80$ mm. The velocity along the X axis direction changes slightly, that is, the velocity in the same radius fluctuates slightly, and the axial velocity gradient varies little, indicating that the velocity distributes evenly in the flow field, and the velocity and radius of the six cross sections are of linear changes generally.

5.4. Static pressure distribution

Fig. 7 shows the static pressure distribution diagram when the flow is stable, and the internal static pressure of the flow field increases along the radial direction from the material inlet to the places near the drum wall with larger changing amplitude, and reaches the maximum static pressure near the drum wall with most kinetic energy converted to pressure energy. The static pressure along the X axis direction varies little, namely, the fluctuation in the same radius is very small and the axial pressure gradient varies little, indicating that the static pressure distributes evenly in the flow field.

Six cross sections are taken along the radius R, namely $y_1 = 30$ mm, $y_2 = 40$ mm, $y_3 = 50$ mm, $y_4 = 6\,0$mm, $y_5 = 70$ mm and $y_6 = 80$ mm. As shown in Fig. 7, the static pressure in six cross sections and the radius is correlated forming a parabola curve.

5.5. Turbulent kinetic energy and turbulence intensity distribution

The turbulence intensity is the ratio of standard deviation of changing turbulence intensity to the mean velocity, and is the relative index to measure the turbulence intensity. The turbulent kinetic energy is an index to measure the development or decline of turbulent flow, from which it can

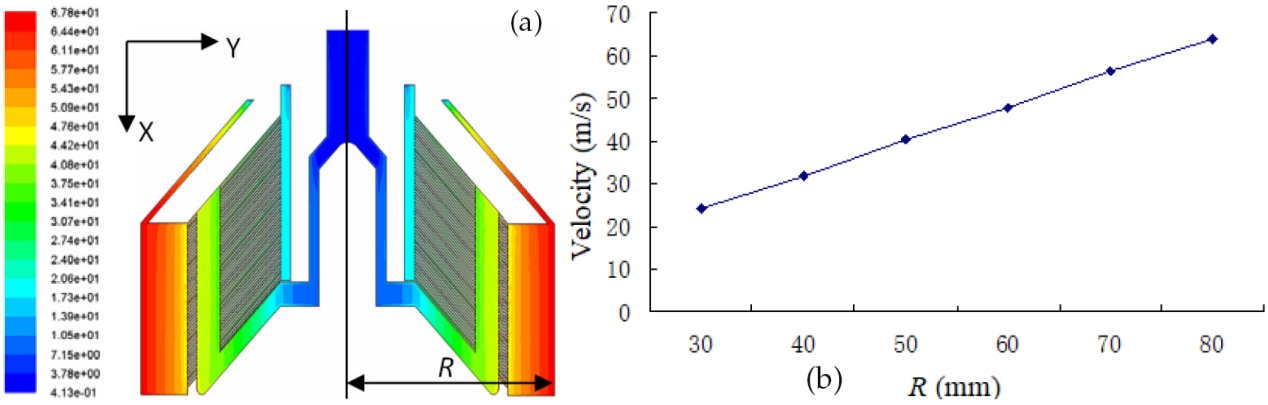

Fig. 6. Velocity distribution diagram when the flow field was stable.

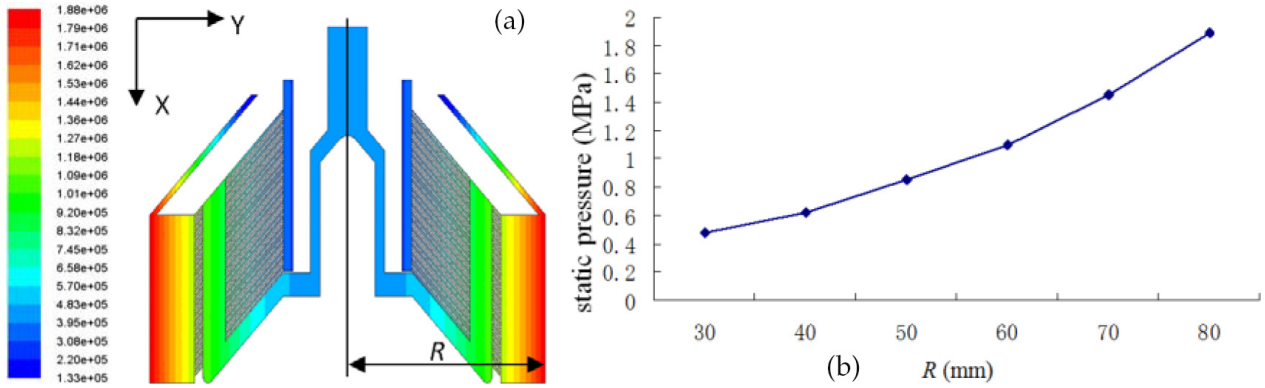

Fig. 7. The static pressure distribution diagram when the stream field is stable.

be more accurate to judge whether there is turbulence in the flow, and it is considered to have a larger turbulence flow when turbulence intensity $k > 10\%$.

Figs. 8 and 9 show the turbulence intensity and turbulent kinetic energy distribution diagram when the flow is stable. There are large turbulence in the material inlet, the disc edge, the edge of neutral hole, the oil outlet and the water outlet with turbulence intensity more than 10%. The turbulence intensity in the gap between discs is smaller than 3%, belonging to laminar flow, which is consistent with the conclusions described in fluid mechanics.

As shown in Fig. 10, oil and water are going to stratify affected by centrifugal force and the gravity, especially the one at the material inlet. The water settles and moves outward with centrifugal force, resulting in local small turbulence phenomenon, but not very obvious.

From Fig. 11, larger turbulence occurs at the edge of center hole and the inside and outside edge of the disc because of a change in shape. It belongs to laminar flow in the internal disc for the gap between discs is very small. This phenomenon is completely consistent with the theory.

6. Prediction and test analysis on separation performance

In order to study the performance of separator, a test table is constructed shown in Fig. 12. According to DL/T

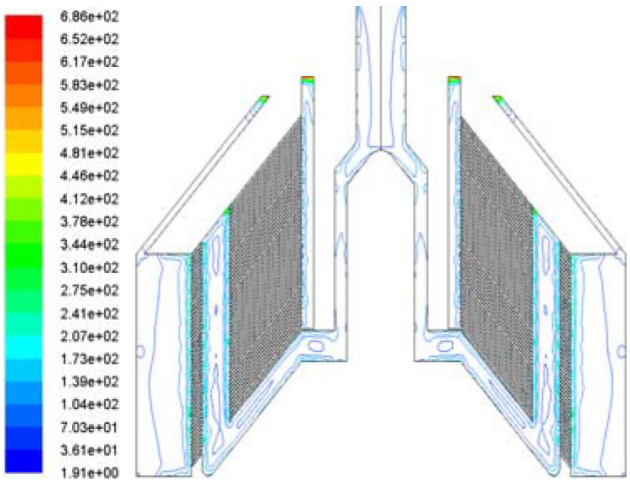

Fig. 8. Turbulence intensity.

432–2007 "Determination of Particulate Contamination in Oil", the automatic particle counting method is used to determine the degree of contamination, and the pollution grade is assessed by the Aerospace Industries Association of America NAS1638 based on the standard of particulate pollution classification, and 8 grade is the required standard level.

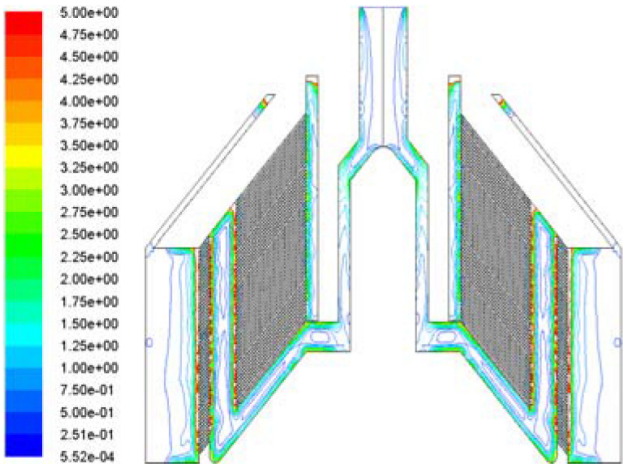

Fig. 9. Turbulent kinetic energy.

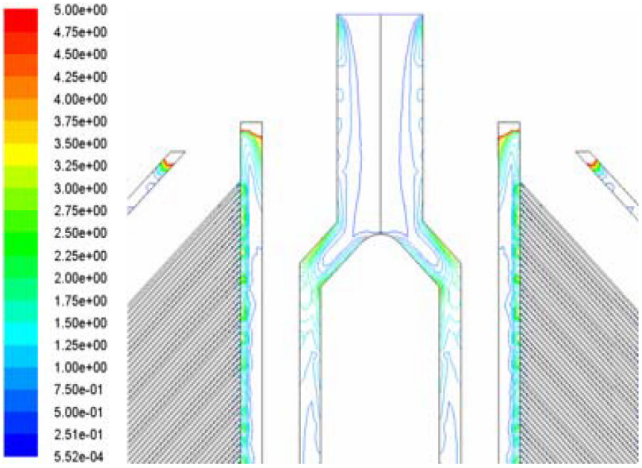

Fig. 10. Turbulent kinetic energy at the inlet

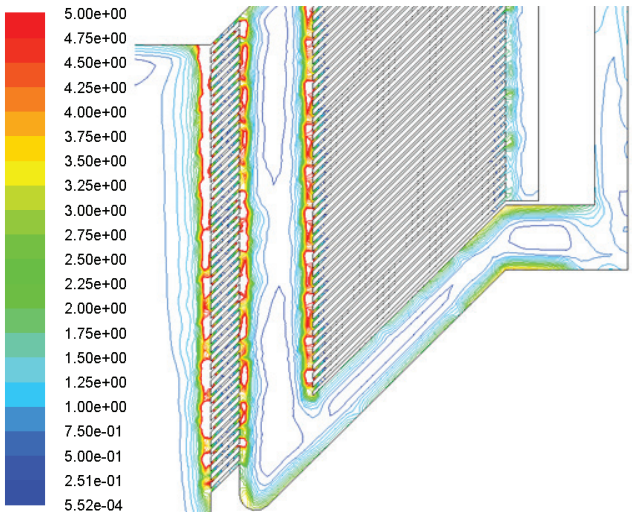

Fig. 11. Turbulent kinetic at the edge of the center hole.

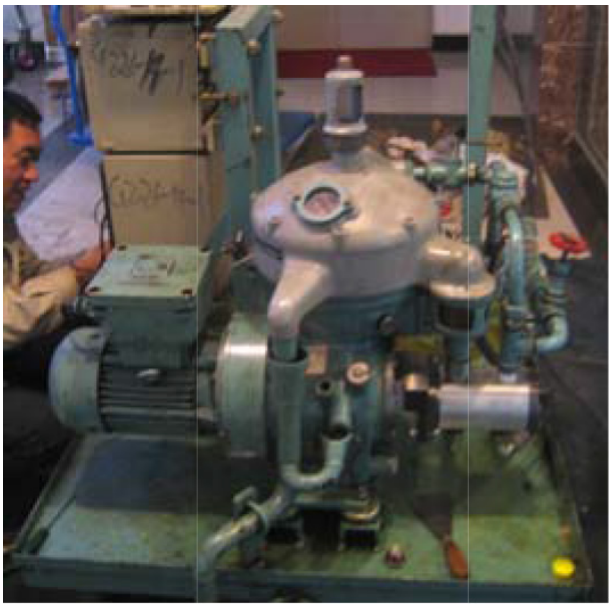

Fig. 12. Separator used in the test

Conduct the performance prediction of lubricating oil separator used in the test under three conditions, Table 3 provides the results of calculating and measured separation efficiency under different conditions, and Fig. 13 shows the comparison between pre-treatment and post-treatment under condition 2.

The numerical simulation and field test show that the separation efficiency of both the calculation and actual measurements meet the design requirements under the design condition 2, and they are quite approximate with the computational separation efficiency slightly higher than the measuring one. The relative error of the oil-water separation efficiency is 1.5% and that of the particle separation efficiency is 1.4%, and the viscosity of lubricant and pour point are quite close to the standard value. All the data indicate that the method adopted in this paper for predicting the separation performance of lubricating oil separator is of higher accuracy.

7. Conclusion

1) A recycling technological process of wastewater treatment for offshore oilfield combining with engineering practice was produced. Analysis method for an unsteady flow field of "oil-water-solid" three-phase flow was presented in this paper. Oil-water separation adopted VOF multiphase flow model, and oil-water-solid phase separation chose discrete phase model. The research shows that the method fully reveals the internal flow mechanism in the separator. The mechanism can not only save the computational time and design cost but also simulate the oil-water separating process and efficiency better.

Table 3
The result of the estimating the separation efficiency and the measured separation efficiency

Working condition	Flow m^3/h	Calculated Value		Experimental Value		Relative error	
		Oil-water separation efficiency/%	Particle separation efficiency/%	Oil-water separation efficiency/%	Particle separation efficiency/%	Oil-water separation efficiency	Particle separation efficiency
1	0.8	97.1	96.5	95.0	94.7	2.1%	1.8%
2	1	99.8	98.2	98.3	96.8	1.5%	1.4%
3	1.2	99.9	98.6	98.7	97.5	1.2%	1.1%

Fig. 13. Comparison diagram of pre-treatment and post-treatment under working condition 2.

2) There is a strong turbulence in the disc edge, the neutral hole edge, the oil and the water outlet with turbulence intensity more than 10%, while the turbulence intensity in the gap between discs is smaller than 3%, belonging to laminar flow, that is completely consistent with theory.
3) Under the design condition, the separation efficiency of both the calculation and actual measurements meet the design requirements with the computational separation efficiency slightly higher than the measuring one. The relative error of oil-water separation efficiency and particle separation efficiency are 1.5% and 1.4% respectively. The data indicate that the numerical simulation method is reliable for predicting the separation performance of the separator, and can meet the requirements for engineering application.

Acknowledgment

This research was financially supported by the National Natural Science Foundation of China (Grant No.51675212), Major Project of Natural Science Research in Universities of Jiangsu Province (Grant No. 16KJA460004).

References

[1] Y. Peng, Q. Wu, Research development of waste lubricant oil recycle technology, Guangzhou Chem. Ind., 42 (2014) 28–31.
[2] Y.L. Guo, Process design and efficiency analysis of compressor lubricant recovery, Shangdong Chemical Industry, 45 (2016) 84–85.
[3] Z.Y. Han, Y.C. Jin, Study on the recovery technology of used lubricating oil of vehicle with acid-free method, Contemp. Chem. Ind., 44 (2015) 1165–1168.
[4] Q.W. Yang, W.Y. Chen, Study on the regeneration of waste lubricating oil, Appl. Chem. Ind., 46 (2017) 1401–1404.
[5] Y.H. Li, J.J. Wu, G.Q. Jiang, H.J. Wu, Y.N. Huai, W.B. Zhao, Progresses in regeneration technologies for used lube oils, Petrochem. Technol., 45 (2016) 244–250.
[6] Z.G. Zhao, B.Q. Shi, Y. Li, Research on analysis of separation efficiency and numerical simulation of inner flow in lubricant separator, Trans. Chinese Soc. Agric. Eng., 27 (2011) 163–168.
[7] S.Z. Wang, Y.Z. Zhang, W.J. Li, Z.J. Lv, L.H. Liang, Comparison of wireless testing and simulation of disc separator drum stress, J. Mech. Elect. Eng., 34 (2017) 740–744.
[8] X.N. Xue, K. Shi, Fluid dynamics characteristic of high-speed drum for latex separator, Trans. Chinese Soc. Agric. Eng., 33 (2017) 279–286.
[9] W.D. Shi, Y. Yang, Verification of comparability and analysis of inner flow fields on scaling models of submersible well pump, Trans. Chinese Soc. Agric. Eng., 33 (2017) 50–57.
[10] H. Li, B. Jiang, T.Q. Lu, Visualization Experiment of Gas-liquid Two-phase Flow of Pump during Self-priming Process, Trans. Chinese Soc. Agric. Machinery, 46 (2015) 59–65.
[11] H. Wu, Analysis on separation efficiency of two kinds of oil-gas separator based on FLUENT, Comp. Aided Eng., 25 (2016) 52–56.
[12] H. Tang, P. Sun, W.F. Liu, Numerical study on the influence of working conditions on separation efficiency of an axial flow cyclone separator, J. Mech. Eng., 53 (2017) 157–163.
[13] G. Macias, C. Cuerda, D. Diaz, Application of the Rosin-Rammler and Gates-Gaudin-Schuhmann models to the particle size distribution analysis of agglomerated cork, Mater. Charact., 52 (2004) 159–164.